



# Mutation in the Disordered Linker Region of Capsid Disrupts Viral Kinetics of a Neuropathogenic SIV in Rhesus Macaques

Cheri A. Lee,<sup>a</sup> Vanessa M. Hirsch<sup>a</sup>

<sup>a</sup>Laboratory of Molecular Microbiology, National Institute of Allergy and Infectious Diseases, National Institutes of Health, Bethesda, Maryland, USA

**ABSTRACT** TRIM5 $\alpha$  polymorphism in rhesus macaques (RM) limits the genetic pool of animals in which we can perform simian immunodeficiency virus (SIV) studies without first screening animals for permissive TRIM5 $\alpha$  genotypes. We have previously shown that polymorphisms in the TRIM5 $\alpha$  B30.2/SPRY domain impact the level of SIVsmm viremia in RM and that amino acid substitutions (P37S/R98S) in the capsid N-terminal domain (CA-NTD) enables the virus to overcome restriction in RMs with the restrictive homozygous TRIM5 $\alpha$ <sup>TFP/TFP</sup> genotype. Since this genotype also negatively impacted the development of central nervous system (CNS) lesions in animals infected with the parental source of CL757, we sought to generate a TRIM5 $\alpha$ <sup>TFP/TFP</sup>-resistant clone, SIV-804E-CL757-P37S/R98S (CL757-SS), using a similar strategy. Unexpectedly, viral replication of CL757-SS was impaired in RMs with either the permissive TRIM5 $\alpha$ <sup>TFP/Q</sup> or the restrictive TRIM5 $\alpha$ <sup>TFP/TFP</sup> genotype. Analysis of the virus which emerged in the latter animals led to the discovery of a preexisting mutation relative to other SIVs. This P146T substitution in a conserved disordered linker region in the C-terminal domain of capsid (CA-CTD) has been shown to inhibit proper formation of HIV-1 capsid particles. Restoration of this residue to proline in the context of the TRIM5 $\alpha$ -SS escape mutations not only restored viral replication, but also enhanced the infectivity of our previously reported neurotropic clone, even in RMs with permissive TRIM5 $\alpha$  genotypes.

**IMPORTANCE** SIV infection of rhesus macaques has become a valuable model for the development of AIDS vaccines and antiretroviral therapies. Polymorphisms in the rhesus macaque TRIM5 $\alpha$  gene can affect SIV replication, making it necessary to genetically screen macaques for TRIM5 $\alpha$  alleles that are permissive for SIV replication. This limits the pool of animals that can be used in a study, thereby making the acquisition of animals needed to fulfill study parameters difficult. We have constructed a viral clone that induces neuroAIDS in rhesus macaques regardless of their TRIM5 $\alpha$  genotype, while also highlighting the important role the disordered linker domain plays in viral infectivity.

**KEYWORDS** TRIM5 $\alpha$ , capsid, disordered linker, *gag*, HIV, neuroAIDS, rhesus macaques, simian immunodeficiency virus, viral infectivity, viral kinetics

Simian immunodeficiency virus (SIV)-infected rhesus macaques (RM) have served as an important model for HIV/AIDS pathogenesis. The HIV epidemic is the result of cross-species transmission of SIV from nonhuman primates (NHP) to humans despite the many restriction factors that exist in humans to block SIV transmission (1, 2). What makes rhesus macaques a desirable model for HIV/AIDS pathogenesis studies is that, once infected with SIV, their disease progression is similar to that of HIV-infected patients, consisting of robust and chronic viral replication and depletion of CD4<sup>+</sup> T cells, which leads to immunodeficiency and opportunistic infections (3). Clinical outcomes vary in HIV-infected individuals in part due to genetic differences in the host immune response, including major homology class I (MHC-I) genes and interferon-inducible, intrinsic restriction factors such as APOBEC3G and tripartite motif-containing

**Editor** Takamasa Ueno, Kumamoto University

This is a work of the U.S. Government and is not subject to copyright protection in the United States. Foreign copyrights may apply.

Address correspondence to Vanessa M. Hirsch, [vhirsch@nih.gov](mailto:vhirsch@nih.gov).

The authors declare no conflict of interest.

**Received** 15 February 2022

**Accepted** 19 February 2022

**Published** 17 March 2022

protein 5 $\alpha$  (TRIM5 $\alpha$ ). The latter genes also are implicated as barriers to cross-species transmission (2, 4–13). Indeed, TRIM5 $\alpha$  was first identified as the protein responsible for host restriction of HIV-1 in rhesus macaque cells. TRIM5 $\alpha$  dimers create a lattice around the lentiviral capsid, which results in disassociation of the viral core prior to reverse transcription (14). While polymorphisms in human-TRIM5 $\alpha$  do not appear to impact disease progression in HIV-infected patients, polymorphisms in the rhesus-TRIM5 $\alpha$  gene have been shown to influence SIVsmm replication in rhesus macaques (8, 9). All domains of TRIM5 $\alpha$  are required for retroviral restriction activity, but the B30.2/SPRY (SPRY) domain is required for specific recognition of capsid (15–21). Insertions or deletions in the SPRY domain are associated with differences in inhibition of SIV viral kinetics in the macaque. Although there are numerous polymorphisms in rhesus TRIM5 $\alpha$ , these can be summarized into three functional TRIM5 $\alpha$  alleles which differ in the SPRY domain and have been designated TRIM5 $\alpha^Q$ , TRIM5 $\alpha^{TFP}$ , and TRIM5 $\alpha^{CYP}$  (22, 23). Of these three alleles, TRIM5 $\alpha^Q$  is permissive for SIVsmm viral replication, whereas TRIM5 $\alpha^{CYP}$  and TRIM5 $\alpha^{TFP}$  are both restrictive. In SIVsmmE543-3 (E543-3)-infected RMs, the viral loads in animals with TRIM5 $\alpha^{TFP/TFP}$  and TRIM5 $\alpha^{TFP/CYP}$  genotypes were 2 to 3 logs lower than those in RMs with at least one permissive TRIM5 $\alpha^Q$  allele (8). E543-3 escaped restriction after passage through macaques with the restrictive TRIM5 $\alpha^{TFP/TFP}$  genotype. Two single amino acid mutations, P37S and R93S, found in the capsid N-terminal domain (CA-NTD), as well as amino acid substitutions 87 to 91 in the CypA binding loop (GPLPA), also in the CA-NTD, were identified as being associated with escape from TRIM5 $\alpha^{TFP}$  and TRIM5 $\alpha^{CYP}$  alleles, respectively (8). Introduction of the P37S and R93S amino acid substitutions to E543-3 and the related viral strain SIVsmmE660 (E660) allowed for better virus acquisition and more efficient replication in the presence of the restrictive TRIM5 $\alpha^{TFP/TFP}$  genotype following repetitive intrarectal challenge (24).

We recently derived an infectious clone, SIVsmm804E-CL757 (CL757), which induces neuroAIDS in 50% of RMs 6 to 12 months after intravenous inoculation (25). As with both E543-3 and E660, TRIM5 $\alpha^{TFP/TFP}$  negatively impacted virus replication and ultimately the development of neuroAIDS in RMs inoculated with the uncloned parental strains used to derive CL757 (12). Therefore, RMs were screened for the absence of the TRIM5 $\alpha^{TFP/TFP}$  genotype, and only animals that were either heterozygous or homozygous for the permissive TRIM5 $\alpha^Q$  allele were inoculated.

In this current study, we introduced the P37S and R93S (SS) single amino acid mutations to our neurotropic clone, CL757. After addition of the SS mutations to the capsid of the neurotropic clone (CL757-SS), we intravenously inoculated naive Indian RMs that were homozygous for TRIM5 $\alpha^{TFP/TFP}$  as well as animals heterozygous for TRIM5 $\alpha^{TFP/Q}$  as controls. We anticipated that the SS substitutions would have a neutral impact on viral kinetics in the permissive TRIM5 $\alpha^{TFP/Q}$  RM but would rescue virus replication in the restrictive TRIM5 $\alpha^{TFP/TFP}$  animals. Unexpectedly, we observed marked impairment of viral replication in all animals inoculated with the CL757-SS virus, although virus eventually emerged at later time points postinoculation. We therefore investigated the capsid sequences of these escape variants. Sequence analysis of emerging viruses led to the discovery of a previously overlooked substitution in CL757-WT (wild type) capsid relative to all other SIV isolates. This amino acid was the target of site-specific substitutions in virus emerging from animals inoculated with CL757-SS. Interestingly, this substitution in CL757-WT, P146T, lies in a highly conserved disordered linker domain of SIV-capsid which has been shown to be critical for the proper formation of the HIV-1 capsid structure (26, 27). Our study investigated the role of this unique capsid substitution in the context of TRIM5 $\alpha$ -escape substitutions, with the goal of producing a clone capable of robustly replicating and uniformly inducing neuroAIDS in macaques of all TRIM5 $\alpha$  genotypes. This clone is of considerable interest to the HIV CURE field, since it would be useful for studying the effect of antiretroviral therapy (ART) on the viral reservoir in the central nervous system. Clearly, the feasibility of such studies would be improved if TRIM5 $\alpha$  genotyping could be avoided; thus, our goal was to generate a variant of CL757 that would not be significantly impacted by TRIM5 $\alpha$  restriction.

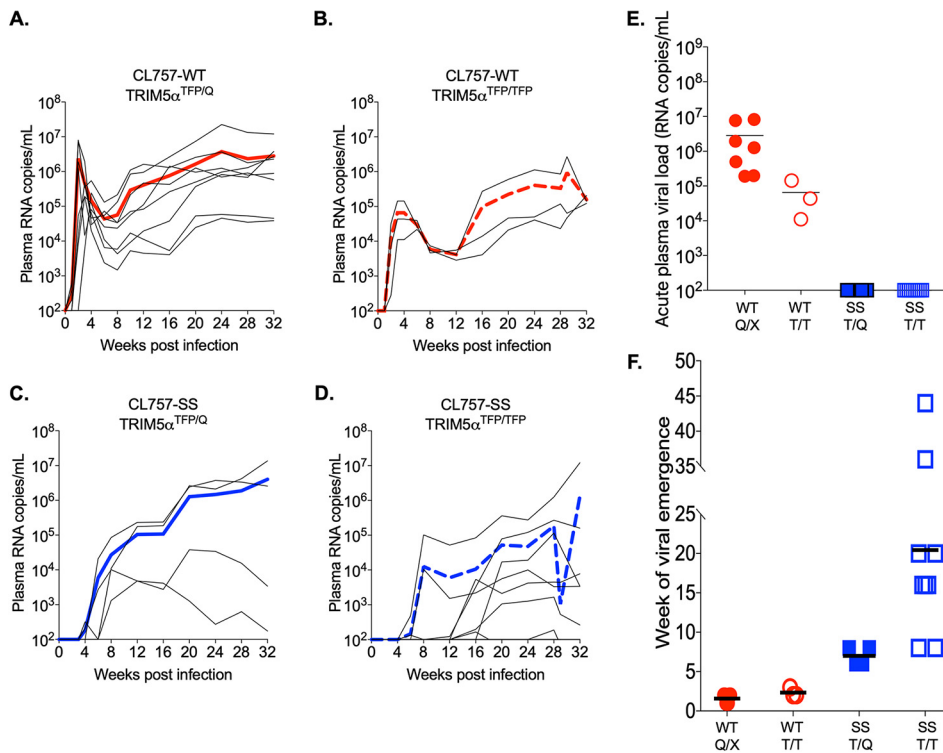


**FIG 1** *In vivo* replication kinetics of CL757-SS in both TRIM5 $\alpha^{TFP/Q}$  and TRIM5 $\alpha^{TFP/TFP}$  rhesus macaques (RM) is severely delayed. (A) Historical animals with TRIM5 $\alpha^{TFP/Q}$  infected with CL757-WT are being used as a reference group for viral kinetics ( $n = 8$ ). (B) First control group is macaques with TRIM5 $\alpha^{TFP/TFP}$  inoculated with CL757-WT ( $n = 3$ ). (C) Second control group consists of TRIM5 $\alpha^{TFP/Q}$  RMs infected with CL757-SS ( $n = 4$ ). (D) The test group is TRIM5 $\alpha^{TFP/TFP}$  RMs infected with CL757-SS ( $n = 9$ ). Bolded lines represent average replication curves for each group. (E) Comparison of acute plasma viral load levels for each animal group. (F) Week at which virus first emerged for each animal in their respective groups. Red color indicates CL757-WT-infected animals and blue indicates for CL757-SS-infected animals. Solid lines, circles, and squares indicate TFP/Q and Q/X RMs. Dashed lines, open squares, and open circles indicate TFP/TFP RMs.

## RESULTS

**SS capsid mutations debilitate CL757 viral kinetics *in vivo*.** The purpose of this study was to generate a variant of our neurotropic CL757 clone with improved viral replication and neuroAIDS induction in rhesus macaques (RM) with the restrictive TRIM5 $\alpha^{TFP/TFP}$  genotype. Prior studies have been successful in overcoming TRIM5 $\alpha^{TFP/TFP}$  restriction by the substitution of serines at positions 37 and 98 in the viral capsid; therefore, we chose to introduce these substitutions into CL757 to generate CL757-P37S/R98S (CL757-SS). This strategy was successful in E660 despite additional substitutions in the cyclophilin A binding loop of capsid relative to E543-3, so we were confident that similar substitutions in the CL757 capsid were unlikely to interfere with this strategy.

We chose to compare the viral kinetics from a historical study in which RMs with at least one permissive TRIM5 $\alpha^Q$  allele were infected with CL757-WT (wild type;  $n = 8$ ) (Fig. 1A) (25). As the first control group, RMs with the TRIM5 $\alpha^{TFP/TFP}$  genotype ( $n = 9$ ) were inoculated with CL757-WT (Fig. 1B); for the second control group, RMs with TRIM5 $\alpha^{TFP/Q}$  genotype ( $n = 4$ ) were inoculated with CL757-SS (Fig. 1C); and for the test group ( $n = 9$ ), RMs with TRIM5 $\alpha^{TFP/TFP}$  were inoculated with CL757-SS (Fig. 1D).

The reference group (CL757-WT-infected-TRIM5 $\alpha^Q$ , TRIM5 $\alpha^{Q/Cyp}$ , and TRIM5 $\alpha^Q/TFP$  RMs [TRIM5 $\alpha^{Q/X}$ ]) showed the typical viral kinetics that have been observed for many other SIV clones (Fig. 1A): acute viral peaks at around 10<sup>7</sup> RNA copies/mL (Fig. 1E) at 2 weeks postinfection (Fig. 1F), with establishment of a set point starting by 8 to 12 weeks. RMs of the restrictive TRIM5 $\alpha^{TFP/TFP}$  genotype inoculated with CL757-WT exhibited similar viral kinetics (Fig. 1B); however, the acute peak viral load was 1 to 2 logs lower and was slightly delayed compared to that in RMs from the permissive

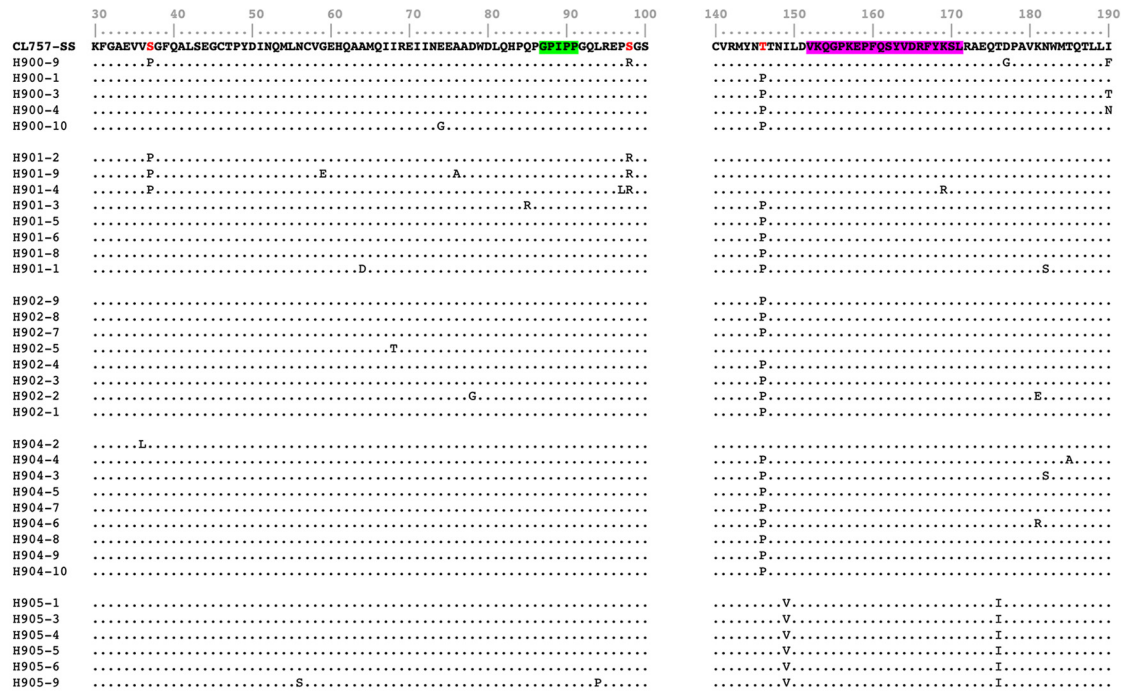
TRIM5 $\alpha^{Q/X}$  reference group (Fig. 1E). This difference is presumably due to the restrictive nature of the homozygous TFP genotype. We then evaluated the effect of introducing SS mutations into the capsid of CL757 following intravenous inoculation of CL757-SS into RMs with a permissive TRIM5 $\alpha^{TFP/Q}$  genotype ( $n = 4$ ) (Fig. 1C) and RMs with a restrictive TRIM5 $\alpha^{TFP/TFP}$  genotype ( $n = 9$ ) (Fig. 1D). The introduction of the SS mutation should have rescued viral kinetics in the TRIM5 $\alpha^{TFP/TFP}$  RMs and have no effect on virus replication in permissive TRIM5 $\alpha^{TFP/Q}$  RMs. However, we instead observed a significant delay in viral emergence and a loss of an acute viral peak even in the supposedly permissive TRIM5 $\alpha^{TFP/Q}$  RMs (Fig. 1C and E), and an even more severe delay of viral emergence and the near absence of acute viral peak in TRIM5 $\alpha^{TFP/TFP}$  RM infected with CL757-SS (Fig. 1D and E). The delay in emergence of virus in plasma ranged from 8 to 45 weeks following inoculation (Fig. 1F). This pattern of viral kinetics is characteristic of an initial significant block to viral replication and the subsequent generation of escape mutations.

**Identification of a T146P mutation in the SIV-CL757 capsid.** We examined the viral capsid sequence in plasma virus of RM inoculated with CL757-SS to confirm the persistence of the SS substitutions and identify escape mutations that could be responsible for the late emergence of virus. We first evaluated CL757-SS-infected TRIM5 $\alpha^{TFP/TFP}$  macaques, as these animals had the most severe delay in virus emergence (Fig. 1F). Viral RNA was isolated from plasma on the day of recorded viral emergence from each animal. Bulk sequencing confirmed the retention of the SS mutation in the viral capsid; however, a consistent mutation relative to CL757-WT appeared at position 146 in the capsid (Fig. 2A). Thr-146 had changed to Pro in every RM except for H905, which instead had the substitutions Val-149 and Iso-175 on either side of the major homology region (MHR) (Fig. 2A). This analysis is consistent with a neutral to beneficial impact of the SS substitutions in TRIM5 $\alpha^{TFP/TFP}$  macaques but a deleterious effect of Thr146, at least in the context of the SS substitutions. Analysis of macaques with the permissive TRIM5 $\alpha$  genotype (CL757-SS-infected TRIM5 $\alpha^{TFP/Q}$  RMs) showed a mixed outcome for the inserted SS mutation. Two of the animals sequenced retained the SS mutation and showed similar escape mutants, P146 for animal H906, and mutations in and around the MHR for animal H907 (Fig. 2B), like the substitutions seen in RM with a restrictive TRIM5 $\alpha$  genotype. However, the other two animals showed either a complete loss of the SS mutation (H908) or a retention of the S-98 mutation and the escape mutation at position 146 with either Ala or Ser in place of the Thr. Overall, these data suggested that the SS mutations were neutral or deleterious in the context of CL757 in RMs with permissive TRIM5 $\alpha$  and that the T146 was the focus of escape mutations.

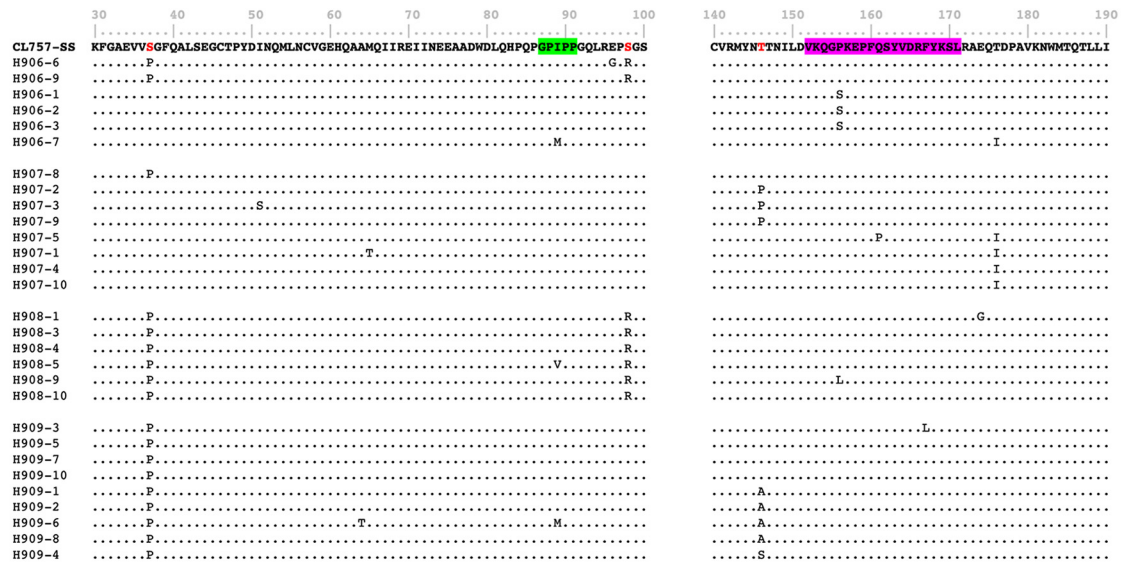
We next evaluated peak plasma viral sequences in CL757-WT-inoculated, restrictive TRIM5 $\alpha^{TFP/TFP}$  RMs. These samples showed the same escape mutation appearing at position 146 of the capsid in H898 (Fig. 2C). The pattern of escape mutations was complex and influenced by the presence or absence of the SS substitutions as well as by the TRIM5 $\alpha$  genotype of the animal. However, this evidence supports what we already know about the restrictive nature of the TFP/TFP allele: the SS substitutions have a positive influence on viral replication in CL757-WT-infected RMs with restrictive TRIM5 $\alpha$  genotypes. However, in the context of Thr at position 146, virus replication was impaired, forcing an escape mutation, Thr to Pro, to appear at position 146. The changes to capsid that we had observed in the CypA-binding region of CL757-WT were unaltered in any of the present study animals.

An alignment of the HIV capsid gene and various SIV strains showed that position 146 of the SIV capsid is a conserved proline (Fig. 3A). It has been previously demonstrated that HIV Pro-147 is part of a disordered linker domain which connects the HIV capsid N-terminal domain (CA-NTD) and the capsid C-terminal domain (CA-CTD) (26, 27). Mutations in this domain can result in improper formation of the capsid, leading to a reduction in the number of viable virions produced, and SIV shares a similarly biologically active linker region with HIV (28). The presence of Thr-146 is presumably an error that arose during PCR and cloning, since bulk sequence analysis of the virus

**A. CL757-SS infected TRIM5<sup>TFP/TFP</sup> RMs**



**B. CL757-SS infected TRIM5<sup>TFP/Q</sup> RMs**



**C. CL757-WT infected TRIM5<sup>TFP/TFP</sup> RMs**

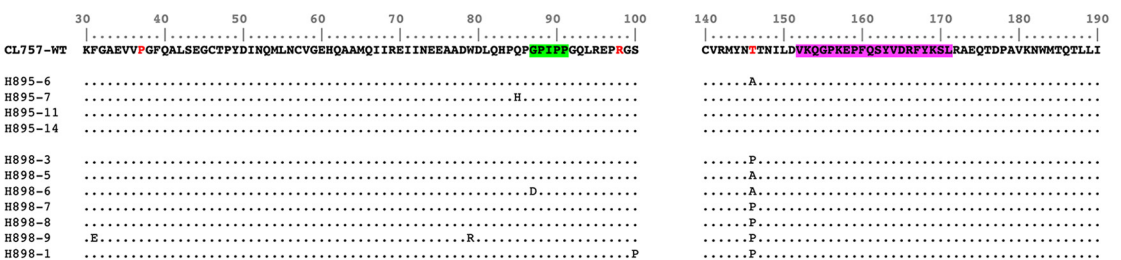


**FIG 2** Partial capsid alignments from plasma virus isolated at time of emergence from each animal, aligned with the respective inoculum. Alignment of capsid mutations found in macaques infected with either CL757-WT or CL757-SS. (A) Test group: CL757-SS- (Continued on next page)

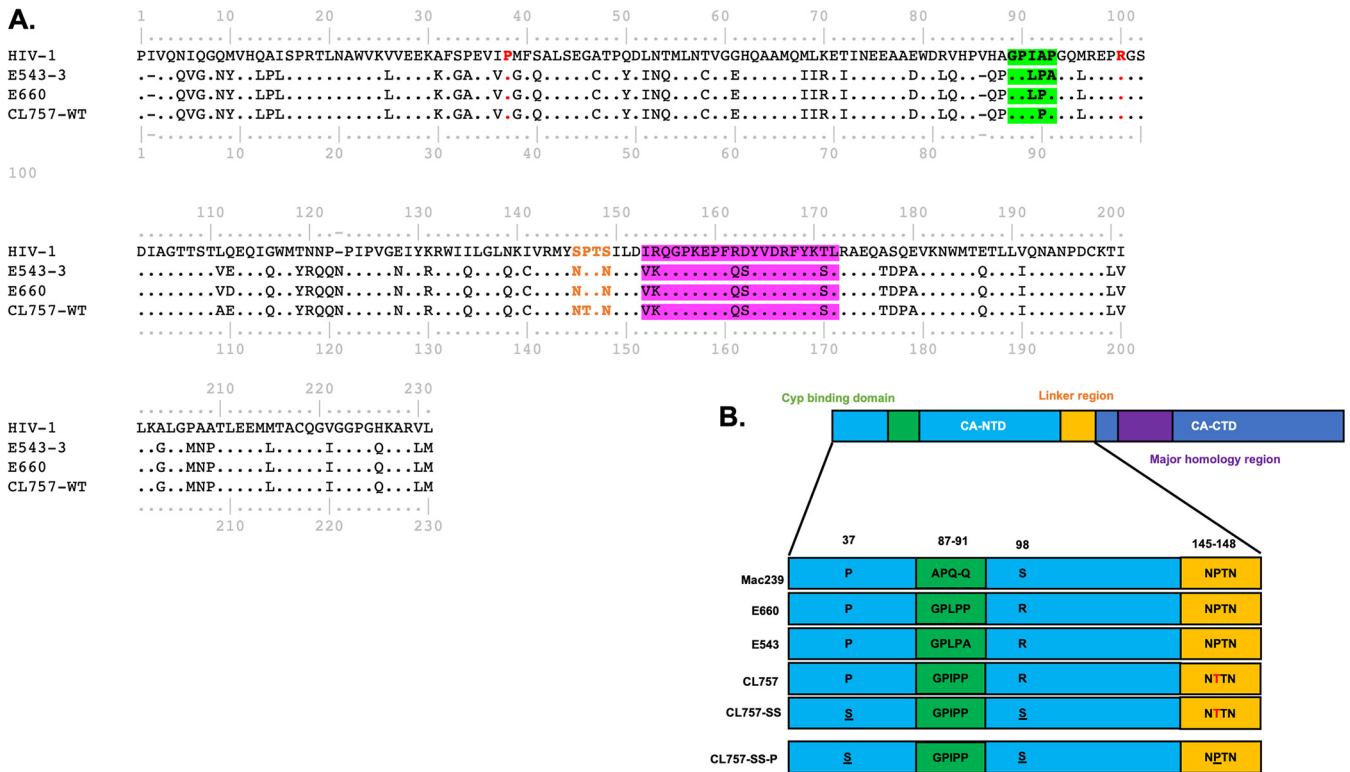


**FIG 3** An alignment of the HIV capsid gene and various SIVsmm strains shows that position 146 of the SIV capsid is a conserved proline. (A) HIV-1, SIVsmm strains E660 and E543-3, and CL757-WT exhibit HIV-P147 and SIVsmm-P146 in the disordered linker domain (orange) which are conserved despite the many differences in sequence between HIV and SIV capsids. SIV P37 and R98 residues (HIV P38 and R100) are highlighted in red. The CypA binding region and MHR are in pink. (B) Cartoon depiction of the organization of the capsid gene aligned with SIVMac239, as well as with SIVsmm strains, with the Thr-146 error in red and the engineered changes to the clone underlined.

isolate that was the source of the CL757 cloned, SIVsmm804E (12), showed that this isolate and additional clones from it encoded a Pro at this site (data not shown). Therefore, what we initially thought was an escape mutation at position 146 appears to be a reversion of a potential PCR error in the original CL757-WT clone. The functional significance of this substitution only became apparent in the context of the SS mutations introduced to remove restriction by TRIM5 $\alpha$ .

**Correction of linker mutation restores viral kinetics *in vitro* and *in vivo*.** Based on the pattern of escape mutations, we restored the linker error in both CL757-WT and CL757-SS clone from T146 back to the highly conserved P146 (CL757-WT-P and CL757-SS-P) found in other SIV clones (Fig. 3B) and first examined viral kinetics *in vitro*. Using peripheral blood mononuclear cells (PBMCs) taken from naive RMs with TRIM5 $\alpha$ <sup>TFP/Q</sup> alleles and TRIM5 $\alpha$ <sup>TFP/TFP</sup> alleles, we saw a restoration of viral replication kinetics compared to the original clones (Fig. 4A and B).

Next, we inoculated naive TRIM5 $\alpha$ <sup>TFP/Q</sup> RMs ( $n = 4$ ) and naive TRIM5 $\alpha$ <sup>TFP/TFP</sup> RMs ( $n = 4$ ) with CL757-SS-P. Due to the practical limitations of comparing virus replication and pathogenesis of multiple combinations of mutations in two different genotypes of RM, we chose to focus on the clone that would be of most benefit to the field. We observed restoration of viral kinetics *in vivo* in both TRIM5 $\alpha$ <sup>TFP/Q</sup> and TRIM5 $\alpha$ <sup>TFP/TFP</sup> RMs (Fig. 5A and B). In addition, we saw a higher acute viral load in TRIM5 $\alpha$ <sup>TFP/Q</sup> RMs

**FIG 2 Legend (Continued)**

infected TRIM5 $\alpha$ <sup>TFP/TFP</sup> RMs with the appearance of a mutation, T146P, in all animals infected; except for H905, which has different escape mutations, 1145V and T175I, located outside the major homology region (MHR, pink). (B) Second control group: CL757-SS-infected TRIM5 $\alpha$ <sup>TFP/Q</sup> RMs, showing a reversion of either the engineered S37 or S98 mutation or both. Also, the T146P mutation appears wherever the S37/S98 mutations were lost. (C) First control group: CL757-WT-infected TRIM5 $\alpha$ <sup>TFP/TFP</sup> RMs, with the T146P mutation appearing here as well. Amino acids of interest are highlighted in red and the CypA binding region in green.

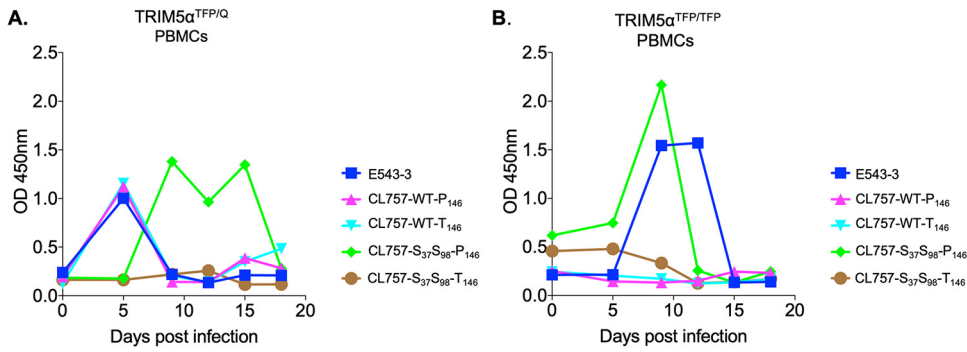


**FIG 4** Correction of the Thr-146 error to Pro restores *in vitro* viral kinetics. Peripheral blood mononuclear cells (PBMCs) were isolated from naive RMs with the genotype (A) TRIM5 $\alpha^{TFP/Q}$  or (B) TRIM5 $\alpha^{TFP/TFP}$ . Cells were infected with multiple iterations of the CL757 clone and viral kinetics were compared to those of the parental clone virus E543-3. Virus output was quantitated by p27 antigen capture assay.

infected with CL757-SS-P compared to the reference group of TRIM5 $\alpha^{Q/X}$  RMs infected with the original CL757-WT (Fig. 5C), and a higher acute plasma viral load in the TRIM5 $\alpha^{TFP/TFP}$  RMs infected with CL757-SS-P relative to TRIM5 $\alpha^{TFP/TFP}$  RMs infected with CL757-WT. The viral peak and emergence at week 2 were restored with the correction of Thr-146 to Pro (Fig. 5D).

Viral load in the cerebrospinal fluid (CSF) helps demonstrate establishment of viral infection in the brain (29). The reference clone CL757-WT, which contained the Thr-146 error, was successful at inducing SIV in half of the TRIM5 $\alpha^{Q/X}$  RMs that were infected (Fig. 6A) (25). The CL757-WT clone successfully established an infection in the central nervous system (CNS) and replicated to high titers in the TRIM5 $\alpha^{Q/X}$  RMs, as indicated by high viral loads in the CSF and the accumulation of multinucleated giant cells in the

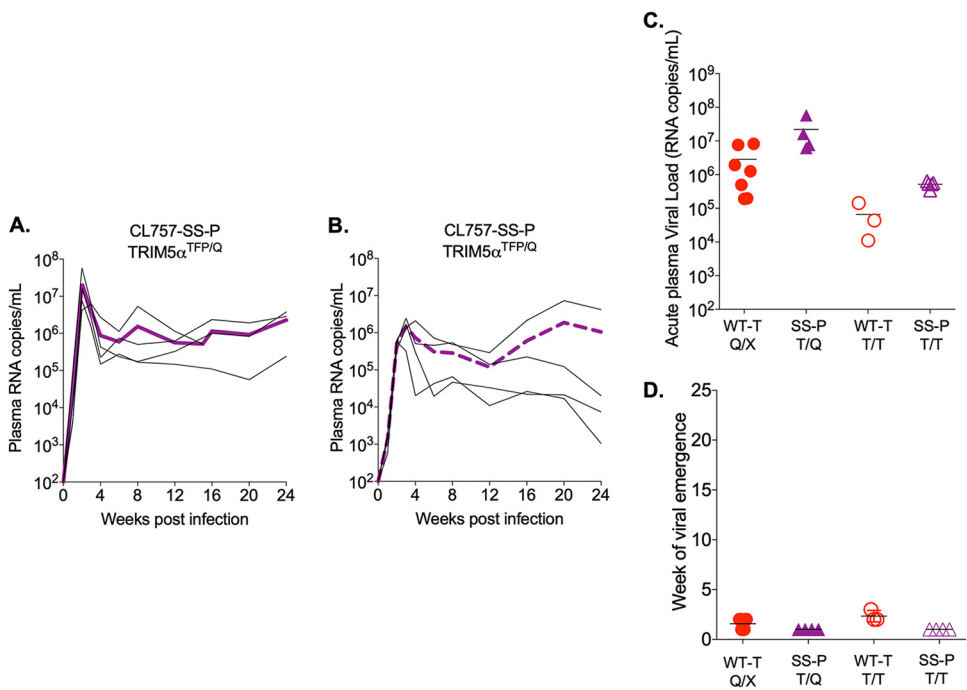


**FIG 5** Correction of the Thr-146 error to Pro restores *in vivo* viral kinetics. (A) TRIM5 $\alpha^{TFP/Q}$  and (B) TRIM5 $\alpha^{TFP/TFP}$  RMs were intravenously inoculated with the corrected clone, CL757-SS-P. (C) Correction of Thr-146 to Pro restores viral kinetics and causes an increase in acute viral load in TRIM5 $\alpha^{TFP/Q}$  RMs compared to that in the reference group. (D) Restoration of proline also eliminates the delay in viral emergence. Bold lines (purple) represent the average replication curve for each group. Red indicates CL757-WT-infected animals and purple indicates CL757-SS-P-infected animals. Solid lines, circles, and triangles indicate TFP/Q RMs. Dashed lines, open circles, and triangles indicate TFP/TFP RMs.

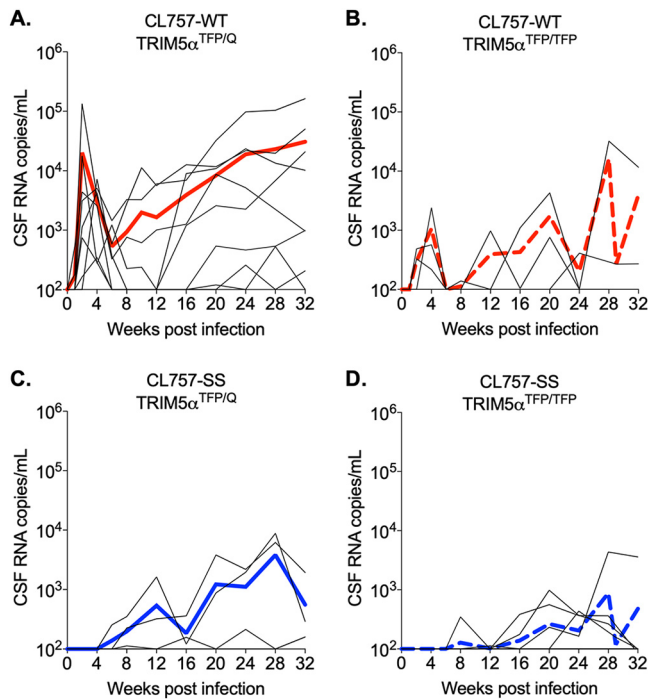


**FIG 6** Cerebrospinal fluid (CSF) viral loads in RMs infected with clones with the error Thr-146. (A) Historical animals with TRIM5 $\alpha^{TFP/Q}$  infected with CL757-WT were used as a reference group for CSF viral kinetics ( $n = 8$ ). (B) First control group is macaques with TRIM5 $\alpha^{TFP/TFP}$  ( $n = 3$ ) inoculated with CL757-WT. (C) Second control groups is TRIM5 $\alpha^{TFP/Q}$  macaques infected with CL757-SS ( $n = 4$ ). (D) The test group is TRIM5 $\alpha^{TFP/TFP}$  macaques infected with CL757-SS ( $n = 9$ ). Bold lines (purple) represent the average replication curve for each group. Red indicates CL757-WT-infected animals and blue indicates CL757-SS-infected animals. Solid lines indicate TFP/Q and Q/X RMs, dashed lines indicate TFP/TFP RMs.

neuroparenchyma (25, 30). TRIM5 $\alpha^{TFP/TFP}$  RMs infected with CL757-WT, as well as TRIM5 $\alpha^{TFP/Q}$  and TRIM5 $\alpha^{TFP/TFP}$  RMs infected with CL757-SS, did not develop neuroAIDS (Fig. 6B to D). CL757-SS-P infection of TRIM5 $\alpha^{TFP/Q}$  RMs led to rapid progression in one animal, H918, which was euthanized due to high CSF viral load and the development of neurological symptoms at 15 weeks postinfection (Fig. 7A). Histopathology of the brain revealed characteristic pathology with glial nodules and the presence of SIV-expressing multinucleated giant cells (data not shown). The other three animals showed persistence of CSF viral loads which approached  $10^5$  RNA copies/mL. Levels greater than  $10^4$  have been previously shown to be associated with productive infection of the CNS (25, 30). At this early stage of the study, it is not possible to determine

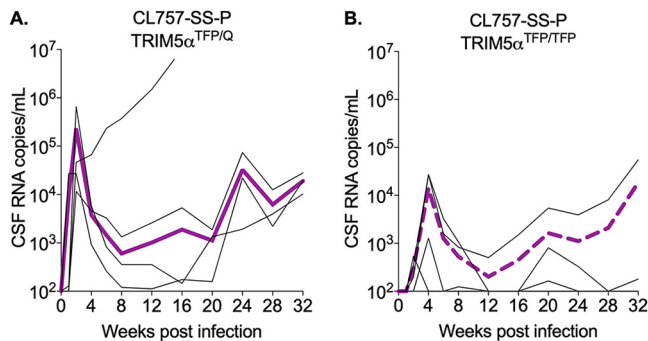


**FIG 7** CSF viral loads in RMs infected with CL757-SS-P (A) TRIM5 $\alpha^{TFP/Q}$  and (B) TRIM5 $\alpha^{TFP/TFP}$  RMs were intravenously inoculated with the corrected clone, CL757-SS-P. Bold lines (purple) represent the average replication curve for each group. Solid lines indicate TRIM5 $\alpha^{TFP/Q}$  RMs, dashed lines indicate TRIM5 $\alpha^{TFP/TFP}$  RMs.



whether CL757-SS-P infection will result in CNS infection and disease in TRIM5 $\alpha$ <sup>TFP/TFP</sup> macaques (Fig. 7B). However, the improved viral replication and development of CNS lesions in the TRIM5 $\alpha$ -permissive RMs in this study indicate that CL757-SS-P is superior to the WT clone in its ability to induce neuroAIDS in the RM model.

## DISCUSSION

In this study, we demonstrated that capsid mutations and TRIM5 $\alpha$  polymorphisms have a significant impact on viral kinetics of SIVsmm molecular clones. We have previously reported on the restrictive role TRIM5 $\alpha$  has in HIV/SIV evolution (7, 8). Using our neurotropic clone which has either an error or a correction in the linker region of the capsid gene, we observed a stark change in viral kinetics and clinical outcomes in TRIM5 $\alpha$ -restrictive RMs (TRIM5 $\alpha$ <sup>TFP/TFP</sup>) versus TRIM5 $\alpha$ -permissive (TRIM5 $\alpha$ <sup>TFP/Q</sup>) macaques. We have previously reported on SIVsmm clones which are sensitive to TRIM5 $\alpha$ -restrictive phenotypes, which led to a 2 to 3 log reduction in acute viral load and the eventual development of escape mutations which rescued viral replication *in vivo* (7–9). Introduction of these two mutations to SIVsmm clones resulted in clones which showed equivalent viral acquisition and replication in TRIM5 $\alpha$ -restrictive and -permissive RMs. In contrast to the findings of these prior studies, addition of the SS mutations to CL757 did not rescue viral replication in the RMs with TRIM5 $\alpha$ <sup>TFP/TFP</sup>, but it nearly abrogated viral replication. This led to the identification of an inherent error in the conserved linker domain of SIV *gag* of the original PCR-generated clone CL757, the correction of which restored and enhanced viral kinetics in the TRIM5 $\alpha$ <sup>TFP/TFP</sup> and TRIM5 $\alpha$ <sup>TFP/Q</sup> macaques, respectively. This study demonstrates that the structural context of TRIM5 $\alpha$  escape mutations introduced into SIV capsids are crucial.

Structural studies of HIV capsid have shown a flexible linker domain (residues 146 to 150) that allows for movement of the CA-CTD relative to the CA-NTD (31–34) and have shown that the linker becomes more structured upon multimerization of the capsid (35). Studies introducing mutations into the linker domain led to a defect in virus assembly as well as virions with abnormal morphology (26, 27). Jiang et al. (26) substituted amino acids throughout the linker domain, and while most of the substitutions lead to noninfectious virions and defects in core assembly, the mutant P147L was of most interest to us, because it affected an amino acid residue homologous to that of our SIV CL757 (P146T) and had a similar phenotype. They reported that HIV-1 P147L is “. . .poorly infectious, [and has] a novel attenuated phenotype.” We see evidence of this phenotype in the original CL757-WT *in vivo* infection of TRIM5 $\alpha$ <sup>Q/X</sup> macaques when viral replication is compared to that in CL757-SS-P infection of TRIM5 $\alpha$ <sup>TFP/Q</sup> macaques (Fig. 5). We observe a moderately reduced viral titer in CL757-WT-infected TRIM5 $\alpha$ <sup>Q/X</sup> RMs compared those of other pathogenic clones of SIVsmm, such as E543-3, which was overlooked until its replication was compared to that in CL757-SS-P-infected TRIM5 $\alpha$ <sup>TFP/Q</sup> RMs. Granted, the comparison of CL757-WT infection of the reference group with CL757-SS-P infection of TRIM5 $\alpha$ <sup>TFP/Q</sup> RMs was not an ideal comparison for two reasons: (i) animals in the reference group had various TRIM5 $\alpha$  genotypes, and (ii) a direct comparison of clones with and without the P146T mutation, without the additional SS mutations, would have been more informative. However, comparing viral replication and pathogenesis of multiple combinations of mutations in two different RM genotypes was impractical, and we instead chose to focus on the clone that would be of most benefit to the field: CL757-SS-P, a virus with the potential to replicate and produce CNS disease in all TRIM5 $\alpha$  genotypes of macaques. Such a clone would be particularly critical for studies of viral reservoirs in the presence and absence of ART therapy.

The effect of the SIV capsid error Thr-146 in the presence and absence of TRIM5 $\alpha$ -escape mutations in *gag* suggest that this residue has a deleterious effect on virus replication. The finding of abnormal core formation in HIV-1 variants encoding a similar substitution at the homologous residue is consistent with shared effects on SIV core formation, but clearly would require additional structural and biochemical studies. Jiang et al. (26) reported that HIV-P147L led to a 35% reduction in virus production,

which could potentially account for the 50% of RMs that develop neurotropism when infected with the CL757-WT clone. Correction of the SIV-Thr-146 to Pro led to rapid disease progression in one of the TRIM5 $\alpha$ <sup>TFP/Q</sup> RM. The steadily increasing CSF viral loads observed in the other three CL757-SS-P-infected RMs (Fig. 7A) is also consistent with the establishment of viral replication in the brain (12, 25, 29, 30). These results suggest that the Thr-146 error in CL757-WT could be causing a reduction in the proper formation of viral cores, and therefore, reduced infectivity. Virus replication was also rescued in TRIM5 $\alpha$ <sup>TFP/TFP</sup> RMs, although acute viral loads were 1 log lower than those of their TRIM5 $\alpha$ <sup>TFP/Q</sup> counterparts (Fig. 4C and D). Whether or not CL757-SS-P infection of TRIM5 $\alpha$ <sup>TFP/TFP</sup> RMs leads to neurotropism will require longer-term clinical and virologic follow-up with these macaques.

Interestingly, introduction of the SS mutation to the error-afflicted clone seemed to enhance the defect that was already present. CL757-WT-infected TRIM5 $\alpha$ <sup>TFP/TFP</sup> RMs had decreased replication kinetics compared to those in CL757-WT-infected TRIM5 $\alpha$ <sup>Q/X</sup> RMs (Fig. 1A and B). This was the expected result, given the absence of the SS mutation needed to enable the virus to evade the TFP/TFP alleles; however, when we examined the capsid sequence (Fig. 2C), we saw an escape mutation/correction of the Thr-146 to Pro or Ala in RM H898, indicating that this mutation in the linker region is not well tolerated by TRIM5 $\alpha$ <sup>TFP/TFP</sup> RMs and the addition of the SS mutation further complicated the situation. The evolutionary escape pathway in the study animals was complex and dependent upon the TRIM5 $\alpha$  phenotype of each study animal. Slightly different patterns of evolution were observed in each of the permissive TRIM5 $\alpha$ <sup>TFP/Q</sup> RMs (Fig. 2C). For RMs H906 and H907, the SS mutations were retained but second site substitutions were observed at Thr-146 or residues in or around the MHR (Ala-149 and Iso-176). Another TRIM5 $\alpha$ <sup>TFP/Q</sup> RM retained the Thr-146 but lost the Ser mutations at positions 37 and 98 (Fig. 2B, RM H908). The MHR has been shown to influence HIV-1 Gag assembly (36, 37) suggesting that the presence of escape mutants in and around the SIV-MHR are presumably rescuing Gag assembly, due to the presence of the destabilizing Thr-146 error.

Patterns of evolution in restrictive CL757-SS-infected TRIM5 $\alpha$ <sup>TFP/TFP</sup> RMs were more consistent between individual animals, perhaps because the virus required the SS mutations to replicate in the presence of TRIM5 $\alpha$ <sup>TFP/TFP</sup>. All viral capsid in these animals retained the SS mutations and showed reversion of Thr-146 to Pro or substitutions outside the MHR. The SS has been shown to be necessary to escape TRIM5 $\alpha$ <sup>TFP/TFP</sup>, so the virus retaining the SS mutation in this context makes sense, but there seems to be a negative interaction occurring due to the presence of both SS and Thr-146. The flexible/disordered linker region has been considered to remotely regulate the overall structural dynamics and molecular interactions of Gag (38). How this occurs is not well known but the studies using CL757-SS-T could possibly be used to start to address this issue.

Even with HIV's ability to evade host restriction factors, the discovery of mutations of the residues (P37S, R98S, T146P, and P146T) and how they function or do not function together sheds light on the crucial role capsid assembly plays in viral infection and kinetics in the SIV/rhesus macaque model, especially when it comes to the TRIM5 $\alpha$  phenotype. This discovery elucidates new targets for antivirals and valuable knowledge in the development of primate animal models for HIV/AIDS.

## MATERIALS AND METHODS

**Ethics statement and animal studies.** This study was carried out in strict accordance with the recommendations described in the Guide for the Care and Use of Laboratory Animals of the National Institutes of Health, the Office of Animal Welfare, and the United States Department of Agriculture. Colony-bred rhesus macaques of Indian origin were obtained from the Morgan Island rhesus monkey breeding colony, SC. All animal work was approved by the NIAID Division of Intramural Research Animal Care and Use Committee (IACUC), in Bethesda, MD (Animal Study protocol, LMM-6). The animal facility is accredited by the American Association for Accreditation of Laboratory Animal Care. All procedures were carried out under ketamine anesthesia by trained personnel under the supervision of veterinary staff, and all efforts were made to ameliorate welfare and minimize animal suffering in accordance with

the recommendations of the Weatherall report on the use of nonhuman primates. Animals were housed in adjoining individual primate cages allowing social interactions, under controlled conditions of humidity, temperature, and light (12-h light/12-h dark cycles). Food and water were available *ad libitum*. Animals were monitored twice daily (pre- and post-challenge) and fed commercial monkey chow, treats, and fruit twice daily by trained personnel. Early endpoint criteria, as specified by the IACUC-approved score parameters, were used to determine when animals were to be humanely euthanized.

**Molecular cloning.** Construction of a SIVsmm804E-CL757 (CL757-WT) full-length molecular clone was described previously (25). To construct SIVsmm804E-CL757-S<sub>37</sub>-S<sub>98</sub> (CL757-SS) full-length clone, amino acid substitutions “P37S” and “R98S” were introduced into CL757-WT capsid using a QuikChange II Site-Directed Mutagenesis kit (Agilent) according to the manufacturer’s instructions. The following primer sets were used to introduce mutations: P37S forward, 5′-GGC AGA GGT AGT GTC AGG ATT TCA AGC G-3′; reverse, 5′-CGC TTG AAA TCC TGA CAC TAC CTC TGC C-3′; R98S forward, 5′-GCA. ACT TAG AGA GCC ATC AGG ATC AGA CAT TGC AG-3′; reverse, 5′-CTG CAA TGT CTG ATC CTG ATG GCT CTC TAA GTT GC-3′. Construction of both SIV804E-CL757-P<sub>146</sub> (CL757-P) and CL757-S<sub>37</sub>-S<sub>98</sub>-P<sub>146</sub> (CL757-SS-P) was performed using overlap PCR. CL757-P was created using SIVsmmE543-3 clone as the PCR template (E543-3 capsid is identical to CL757 except for the CypA binding site and Pro-146). The overlap PCR will target the CypA binding region and not Pro-146). The overlap PCR The first PCR product was amplified using a Platinum *Taq* High Fidelity Kit (Thermo Fisher Scientific, Waltham, MA) using the primers Narl-F (5′-TTG GCG CCC GAA CAG GGA CTT-3′) and GPIPP-R (5′-TCT AAG TTG CCC TGG TGG TAT TGG ACC TGG CT-3′). The second PCR product was created with the primers GagApal-R (5′-CGG GCT GTT CTT CAA TGT AG-3′) and GPIPP-F (5′-AGC CAG GTC CAA TAC CAC CAG GGC AAC TTA GA-3′). Both PCR products were gel-purified using a Qiagen gel purification kit and diluted to 1 ng/μL. Two ng of both PCR products was used in the overlap PCR using Narl-F and GagApal-R as primers to make full-length WT-P-PCR product. Both the WT-P-PCR product and the CL757-WT clone were digested using the restriction enzymes Narl and Apal. The digested CL757-WT was also dephosphorylated using Quick CIP (New England BioLabs). The clone and WT-P-PCR product were ligated together using T4 DNA Ligase (New England BioLabs). The clone CL757-SS-P was also created by overlap PCR using the same procedure as above, but instead using clone SIVsmmE543-3-SS (24) as a template for the first PCR product.

**Viral stocks.** SIVsmm804E-CL757-WT (CL757-WT), SIVsmm804E-CL757-P<sub>146</sub> (CL757-P), SIVsmm804E-CL757-S<sub>37</sub>-S<sub>98</sub> (CL757-SS), and SIVsmm804E-CL757-S<sub>37</sub>-S<sub>98</sub>-P<sub>146</sub> (CL757-SS-P) virus stocks were made by transfection of 293T cells. 293T cells were maintained in complete Gibco GlutaMAX Dulbecco’s modified Eagle medium (DMEM) and transfected with 10 μg of the plasmid using the FuGENE 6 transfection reagent (Roche Diagnostics, Indianapolis, IN) as previously described (39). Virus stocks were collected from the supernatants of transfected cells after 48 h and filtered with a 0.22-μm filter. The 50% tissue culture infectivity dose (TCID<sub>50</sub>) of virus stocks was tested on TZM-bl cells (40).

**Genotyping rhesus macaques for polymorphisms in TRIM5α.** Two to five mLs of whole blood was collected from SIV-naive rhesus macaques into non-EDTA tubes. DNA was isolated from PBMCs using the QIAamp DNA Blood Kit (Qiagen, cat. no. 51104). The TRIM5α gene was amplified with a Platinum *Taq* Hi Fidelity Kit (Thermo Fisher Scientific, Waltham, MA) using the primers TRIM5α 782-F (5′-CGT GAC CTT GAA GAA GCC-3′) and TRIM5α 1087-R (5′-GCT TCC CTG ATG TGA TAC-3′). Amplified PCR product was direct-sequenced and analyzed as described previously (22, 41, 42). To distinguish heterozygous TRIM5α animals from homozygous animals, we examined the electropherograms at the codon sites of interest to look for peaks within peaks.

**In vitro viral replication in PBMCs.** PBMCs were isolated from the whole blood of SIV-naive, healthy rhesus macaques, one with the TRIM5α<sup>TFP/TFP</sup> genotype and one with the TRIM5α<sup>TFP/Q</sup> genotype; the cells were then stimulated with 5 μg of phytohemagglutinin (PHA) per mL and 10% interleukin-2 (IL-2) (Advanced Biotechnologies, Columbia, MD) for 72 h and maintained in RPMI 1640 medium containing 10% fetal calf serum (FCS) and 10% IL-2. PBMCs (5 × 10<sup>5</sup> cells) were inoculated with virus at a multiplicity of infection (MOI) of 0.01, and viral supernatant was harvested every 3 days for 21 days. Virus was quantified by SIV p27 Antigen Capture Assay ELISA (enzyme-linked immunosorbent assay; Advanced Bioscience Laboratories, Rockville, MD) according to the manufacturer’s directions.

**In vivo replication.** Naive Indian-origin rhesus macaques (SIV-, simian retrovirus [SRV]-, and simian T cell leukemia virus type 1 [STLV-1]-seronegative) were prescreened for MHC-I and the TRIM5α genotype. None of the animals used in this study expressed MHC-I genotypes that are known to be restrictive to SIVmac239 (i.e., A1\*001, B\*008, B\*017, B\*029) (49 to 53). Of the animals used in this study, 16 expressed the restrictive TRIM5α<sup>TFP/TFP</sup> genotype and 8 expressed the permissive TRIM5α<sup>TFP/Q</sup> genotype. Animals were inoculated intravenously (i.v.) with 500 TCID<sub>50</sub> of CL757-WT or CL757-SS. Plasma and CSF viral RNA loads were monitored periodically. All animals were housed in accordance with American Association for Accreditation of Laboratory Animal Care standards. The investigators adhered to the Guide for the Care and Use of Laboratory Animals and to NIAID Animal Care and Use Committee-approved protocols.

**Viral RNA extraction and bulk PCR sequence analysis of viral capsids.** Plasma was collected from animals every week during the first month postinfection, then every month onward. Viral RNA was extracted from plasma samples at the first emergence of virus, as detected by RTqPCR, using a QIAamp Viral RNA Minikit (Qiagen). The viral RNA was reverse-transcribed using a ThermoScript reverse transcriptase PCR (RT-PCR) system (Invitrogen) and the cDNA primer 3395-R (5′-CCT CCT ACT ATT TTA GGG GT-3′). The *gag* gene was amplified by PCR with Platinum *Taq* DNA polymerase (Invitrogen) and the primers Narl-F (5′-TTG GCG CCC GAA CAG GGA CTT-3′) and GagApal-R (5′-CGG GCT GTT CTT CAA TGT AG-3′), and then subcloned into the pCR4-TOPO vector using a TOPO TA cloning kit (Invitrogen) for sequencing. A minimum of 10 clones were selected for each sample from each macaque, and the complete *gag* gene was sequenced by Eurofins.

## ACKNOWLEDGMENTS

We thank Richard Herbert, Heather Kendall, and Joanna Swerczek of NIHAC for excellent animal care. Funding was mainly provided by the Intramural Program of the National Institute of Allergy and Infectious Diseases. This project has also been funded in part with federal funds from the National Cancer Institute, National Institutes of Health, under contract no. HHSN261200800001E. The content of this publication does not necessarily reflect the views or policies of the Department of Health and Human Services, nor does the mention of trade names, commercial products, or organizations imply endorsement by the U.S. government.

## REFERENCES

- Hahn BH, Shaw GM, De Cock KM, Sharp PM. 2000. AIDS as a zoonosis: scientific and public health implications. *Science* 287:607–614. <https://doi.org/10.1126/science.287.5453.607>.
- Sharp PM, Hahn BH. 2011. Origins of HIV and the AIDS pandemic. *Cold Spring Harb Perspect Med* 1:a006841. <https://doi.org/10.1101/cshperspect.a006841>.
- Lifson JD, Haigwood NL. 2012. Lessons in nonhuman primate models for AIDS vaccine research: from minefields to milestones. *Cold Spring Harb Perspect Med* 2:a007310. <https://doi.org/10.1101/cshperspect.a007310>.
- Goulder PJ, Watkins DI. 2008. Impact of MHC class I diversity on immune control of immunodeficiency virus replication. *Nat Rev Immunol* 8: 619–630. <https://doi.org/10.1038/nri2357>.
- Walter L, Ansari AA. 2015. MHC and KIR Polymorphisms in Rhesus Macaque SIV Infection. *Front Immunol* 6:540. <https://doi.org/10.3389/fimmu.2015.00540>.
- Krupp A, McCarthy KR, Ooms M, Letko M, Morgan JS, Simon V, Johnson WE. 2013. APOBEC3G polymorphism as a selective barrier to cross-species transmission and emergence of pathogenic SIV and AIDS in a primate host. *PLoS Pathog* 9:e1003641. <https://doi.org/10.1371/journal.ppat.1003641>.
- Kirmaier A, Wu F, Newman RM, Hall LR, Morgan JS, O'Connor S, Marx PA, Meythaler M, Goldstein S, Buckler-White A, Kaur A, Hirsch VM, Johnson WE. 2010. TRIM5 suppresses cross-species transmission of a primate immunodeficiency virus and selects for emergence of resistant variants in the new species. *PLoS Biol* 8:e1000462. <https://doi.org/10.1371/journal.pbio.1000462>.
- Wu F, Kirmaier A, Goeken R, Ourmanov I, Hall L, Morgan JS, Matsuda K, Buckler-White A, Tomioka K, Plishka R, Whitted S, Johnson W, Hirsch VM. 2013. TRIM5 alpha drives SIVsmm evolution in rhesus macaques. *PLoS Pathog* 9:e1003577. <https://doi.org/10.1371/journal.ppat.1003577>.
- Wu F, Ourmanov I, Riddick N, Matsuda K, Whitted S, Plishka RJ, Buckler-White A, Starost MF, Hirsch VM. 2015. TRIM5alpha restriction affects clinical outcome and disease progression in simian immunodeficiency virus-infected rhesus macaques. *J Virol* 89:2233–2240. <https://doi.org/10.1128/JVI.02978-14>.
- Lim S-Y, Chan T, Gelman RS, Whitney JB, O'Brien KL, Barouch DH, Goldstein DB, Haynes BF, Letvin NL. 2010. Contributions of Mamu-A\*01 status and TRIM5 allele expression, but not CCL3L copy number variation, to the control of SIVmac251 replication in Indian-origin rhesus monkeys. *PLoS Genet* 6:e1000997. <https://doi.org/10.1371/journal.pgen.1000997>.
- Lim S-Y, Rogers T, Chan T, Whitney JB, Kim J, Sodroski J, Letvin NL. 2010. TRIM5alpha modulates immunodeficiency virus control in rhesus monkeys. *PLoS Pathog* 6:e1000738. <https://doi.org/10.1371/journal.ppat.1000738>.
- Matsuda K, Dang Q, Brown CR, Keele BF, Wu F, Ourmanov I, Goeken R, Whitted S, Riddick NE, Buckler-White A, Hirsch VM. 2014. Characterization of simian immunodeficiency virus (SIV) that induces SIV encephalitis in rhesus macaques with high frequency: role of TRIM5 and major histocompatibility complex genotypes and early entry to the brain. *J Virol* 88: 13201–13211. <https://doi.org/10.1128/JVI.01996-14>.
- Malim MH, Bieniasz PD. 2012. HIV restriction factors and mechanisms of evasion. *Cold Spring Harb Perspect Med* 2:a006940. <https://doi.org/10.1101/cshperspect.a006940>.
- Stremlau M, Owens CM, Perron MJ, Kiessling M, Autissier P, Sodroski J. 2004. The cytoplasmic body component TRIM5alpha restricts HIV-1 infection in Old World monkeys. *Nature* 427:848–853. <https://doi.org/10.1038/nature02343>.
- D'Cruz AA, Babon JJ, Norton RS, Nicola NA, Nicholson SE. 2013. Structure and function of the SPRY/B30.2 domain proteins involved in innate immunity. *Protein Sci* 22:1–10. <https://doi.org/10.1002/pro.2185>.
- Biris N, Yang Y, Taylor AB, Tomashevski A, Guo M, Hart PJ, Diaz-Griffero F, Ivanov DN. 2012. Structure of the rhesus monkey TRIM5alpha PRYSPRY domain, the HIV capsid recognition module. *Proc Natl Acad Sci U S A* 109: 13278–13283. <https://doi.org/10.1073/pnas.1203536109>.
- Stremlau M, Perron M, Welikala S, Sodroski J. 2005. Species-specific variation in the B30.2(SPRY) domain of TRIM5alpha determines the potency of human immunodeficiency virus restriction. *J Virol* 79:3139–3145. <https://doi.org/10.1128/JVI.79.5.3139-3145.2005>.
- Javanbakht H, Diaz-Griffero F, Stremlau M, Si Z, Sodroski J. 2005. The contribution of RING and B-box 2 domains to retroviral restriction mediated by monkey TRIM5alpha. *J Biol Chem* 280:26933–26940. <https://doi.org/10.1074/jbc.M502145200>.
- Nakayama EE, Miyoshi H, Nagai Y, Shioda T. 2005. A specific region of 37 amino acid residues in the SPRY (B30.2) domain of African green monkey TRIM5alpha determines species-specific restriction of simian immunodeficiency virus SIVmac infection. *J Virol* 79:8870–8877. <https://doi.org/10.1128/JVI.79.14.8870-8877.2005>.
- Perez-Caballero D, Hatzioannou T, Yang A, Cowan S, Bieniasz PD. 2005. Human tripartite motif 5alpha domains responsible for retrovirus restriction activity and specificity. *J Virol* 79:8969–8978. <https://doi.org/10.1128/JVI.79.14.8969-8978.2005>.
- Yap MW, Nisole S, Stoye JP. 2005. A single amino acid change in the SPRY domain of human Trim5alpha leads to HIV-1 restriction. *Curr Biol* 15: 73–78. <https://doi.org/10.1016/j.cub.2004.12.042>.
- Newman RM, Hall L, Connole M, Chen G-L, Sato S, Yuste E, Diehl W, Hunter E, Kaur A, Miller GM, Johnson WE. 2006. Balancing selection and the evolution of functional polymorphism in Old World monkey TRIM5alpha. *Proc Natl Acad Sci U S A* 103:19134–19139. <https://doi.org/10.1073/pnas.0605838103>.
- Wilson SJ, Webb BLJ, Maplanka C, Newman RM, Verschoor EJ, Heeney JL, Towers GJ. 2008. Rhesus macaque TRIM5 alleles have divergent antiretroviral specificities. *J Virol* 82:7243–7247. <https://doi.org/10.1128/JVI.00307-08>.
- Wu F, Kirmaier A, White E, Ourmanov I, Whitted S, Matsuda K, Riddick N, Hall LR, Morgan JS, Plishka RJ, Buckler-White A, Johnson WE, Hirsch VM. 2016. TRIM5 alpha resistance escape mutations in the capsid are transferable between simian immunodeficiency virus strains. *J Virol* 90: 11087–11095. <https://doi.org/10.1128/JVI.01620-16>.
- Matsuda K, Riddick NE, Lee CA, Puryear SB, Wu F, Lafont BAP, Whitted S, Hirsch VM. 2017. A SIV molecular clone that targets the CNS and induces neuroAIDS in rhesus macaques. *PLoS Pathog* 13:e1006538. <https://doi.org/10.1371/journal.ppat.1006538>.
- Jiang J, Ablan SD, Derebail S, Hercik K, Soheilian F, Thomas JA, Tang S, Hewlett I, Nagashima K, Gorelick RJ, Freed EO, Levin JG. 2011. The interdomain linker region of HIV-1 capsid protein is a critical determinant of proper core assembly and stability. *Virology* 421:253–265. <https://doi.org/10.1016/j.virol.2011.09.012>.
- Koma T, Kotani O, Miyakawa K, Ryo A, Yokoyama M, Doi N, Adachi A, Sato H, Nomaguchi M. 2019. Allosteric regulation of HIV-1 capsid structure for Gag assembly, virion production, and viral infectivity by a disordered interdomain linker. *J Virol* 93. <https://doi.org/10.1128/JVI.00381-19>.
- Doi N, Koma T, Adachi A, Nomaguchi M. 2019. Role for Gag-CA interdomain linker in primate lentiviral replication. *Front Microbiol* 10:1831. <https://doi.org/10.3389/fmicb.2019.01831>.
- Zink MC, Suryanarayana K, Mankowski JL, Shen A, Piatak M, Spelman JP, Carter DL, Adams RJ, Lifson JD, Clements JE. 1999. High viral load in the cerebrospinal fluid and brain correlates with severity of simian immunodeficiency virus encephalitis. *J Virol* 73:10480–10488. <https://doi.org/10.1128/JVI.73.12.10480-10488.1999>.
- Lee CA, Beasley E, Sundar K, Smelkinson M, Vinton C, Deleage C, Matsuda K, Wu F, Estes JD, Lafont BAP, Brenchley JM, Hirsch VM. 2020. Simian

- immunodeficiency virus-infected memory CD4(+) T cells infiltrate to the site of infected macrophages in the neuroparenchyma of a chronic macaque model of neurological complications of AIDS. *mBio* 11:e00602-20. <https://doi.org/10.1128/mBio.00602-20>.
31. Berthet-Colominas C, Monaco S, Novelli A, Sibai G, Mallet F, Cusack S. 1999. Head-to-tail dimers and interdomain flexibility revealed by the crystal structure of HIV-1 capsid protein (p24) complexed with a monoclonal antibody Fab. *EMBO J* 18:1124–1136. <https://doi.org/10.1093/emboj/18.5.1124>.
  32. Gamble TR, Yoo S, Vajdos FF, von Schwedler UK, Worthylake DK, Wang H, McCutcheon JP, Sundquist WI, Hill CP. 1997. Structure of the carboxyl-terminal dimerization domain of the HIV-1 capsid protein. *Science* 278:849–853. <https://doi.org/10.1126/science.278.5339.849>.
  33. Gitti RK, Lee BM, Walker J, Summers MF, Yoo S, Sundquist WI. 1996. Structure of the amino-terminal core domain of the HIV-1 capsid protein. *Science* 273:231–235. <https://doi.org/10.1126/science.273.5272.231>.
  34. Momany C, Kovari LC, Prongay AJ, Keller W, Gitti RK, Lee BM, Gorbalenya AE, Tong L, McClure J, Ehrlich LS, Summers MF, Carter C, Rossmann MG. 1996. Crystal structure of dimeric HIV-1 capsid protein. *Nat Struct Biol* 3:763–770. <https://doi.org/10.1038/nsb0996-763>.
  35. Lanman J, Lam TT, Barnes S, Sakalian M, Emmett MR, Marshall AG, Prevelige PE. 2003. Identification of novel interactions in HIV-1 capsid protein assembly by high-resolution mass spectrometry. *J Mol Biol* 325:759–772. [https://doi.org/10.1016/S0022-2836\(02\)01245-7](https://doi.org/10.1016/S0022-2836(02)01245-7).
  36. Mammano F, Ohagen A, Höglund S, Göttlinger HG. 1994. Role of the major homology region of human immunodeficiency virus type 1 in virion morphogenesis. *J Virol* 68:4927–4936. <https://doi.org/10.1128/JVI.68.8.4927-4936.1994>.
  37. von Schwedler UK, Stemmler TL, Klishko VY, Li S, Albertine KH, Davis DR, Sundquist WI. 1998. Proteolytic refolding of the HIV-1 capsid protein amino-terminus facilitates viral core assembly. *EMBO J* 17:1555–1568. <https://doi.org/10.1093/emboj/17.6.1555>.
  38. Keul ND, Oruganty K, Schaper Bergman ET, Beattie NR, McDonald WE, Kadirvelraj R, Gross ML, Phillips RS, Harvey SC, Wood ZA. 2018. The entropic force generated by intrinsically disordered segments tunes protein function. *Nature* 563:584–588. <https://doi.org/10.1038/s41586-018-0699-5>.
  39. Wu F, Ourmanov I, Kuwata T, Goeken R, Brown CR, Buckler-White A, Iyengar R, Plishka R, Aoki ST, Hirsch VM. 2012. Sequential evolution and escape from neutralization of simian immunodeficiency virus SIVsmE660 clones in rhesus macaques. *J Virol* 86:8835–8847. <https://doi.org/10.1128/JVI.00923-12>.
  40. Montefiori DC. 2009. Measuring HIV neutralization in a luciferase reporter gene assay. *Methods Mol Biol* 485:395–405. [https://doi.org/10.1007/978-1-59745-170-3\\_26](https://doi.org/10.1007/978-1-59745-170-3_26).
  41. Brennan G, Kozyrev Y, Kodama T, Hu S-L. 2007. Novel TRIM5 isoforms expressed by *Macaca nemestrina*. *J Virol* 81:12210–12217. <https://doi.org/10.1128/JVI.02499-06>.
  42. Newman RM, Hall L, Kirmaier A, Pozzi L-A, Pery E, Farzan M, O'Neil SP, Johnson W. 2008. Evolution of a TRIM5-CypA splice isoform in old world monkeys. *PLoS Pathog* 4:e1000003. <https://doi.org/10.1371/journal.ppat.1000003>.